IEEE Control Systems Letters paper presented at
2023 62nd IEEE Conference on Decision and Control (CDC)
December 13-15, 2023. Marina Bay Sands, Singapore

Continuification control of large-scale multiagent systems under limited sensing and structural perturbations

Gian Carlo Maffettone[1], Maurizio Porfiri[2,†,*], Mario di Bernardo[1,3,†,*]

***Abstract*— We investigate the stability and robustness properties of a continuification-based strategy for the control of large-scale multiagent systems. Within this framework, one transforms the microscopic, agent-level description of the system dynamics into a macroscopic continuum-level, for which a control action can be synthesized to steer the macroscopic dynamics towards a desired distribution. Such an action is ultimately discretized to obtain a set of deployable control inputs for the agents to achieve the goal. The mathematical proof of convergence toward the desired distribution typically relies on the assumptions that no disturbance is present and that each agent possesses global knowledge of all the others' positions. Here, we analytically and numerically address the possibility of relaxing these assumptions for the case of a one-dimensional system of agents moving in a ring. We offer compelling evidence in favor of the use of a continuification-based strategy when agents only possess a finite sensing capability and spatio-temporal perturbations affect the macroscopic dynamics of the ensemble. We also discuss some preliminary results about the benefits of adding an integral action in the macroscopic control solution.**

I. Introduction

Continuification (or continuation) control was first proposed in [1] as a viable approach to control the collective behavior of large-scale multiagent systems. The key idea of continuification consists of three fundamental steps: (i) finding a macroscopic description (typically a partial differential equation, PDE) for the collective dynamics of the multiagent system of interest; (ii) designing a macroscopic control action to attain the desired collective response; (iii) discretize the macroscopic control action to obtain feasible control inputs for the agents at the microscopic level.

This methodology tackles problems in which the control goal is formulated at the macroscopic dynamics level, but control actions can be exerted only at the microscopic agent scale [2]. Applications of the approach are related, but not limited to, multi-robot systems [3]–[6], cell populations [7]–[9], neuroscience [10], [11], and human networks [12], [13].

Such an approach was used in [14] to control the distribution of a multiagent system swarming in a ring, leading to an effective control scheme for the multiagent system to achieve a desired distribution. Crucially, to prove convergence of the macroscopic collective dynamics towards the desired distribution, two key assumptions were made. Firstly, that agents possess unlimited sensing capabilities so as to know the positions of all other agents in the swarm. Secondly, that no disturbance or perturbation is affecting the dynamics.

The aim of this paper is to remove these often unrealistic assumptions and study the performance, stability, and robustness of the continuification approach in the presence of limited sensing capabilities, spatio-temporal disturbances, or perturbations of the agents' interaction kernel. In particular, we prove that semiglobal asymptotic or bounded convergence can still be achieved under these circumstances. As we undertake this task, we offer insights into the role of the control parameters in changing the size and shape of the region of asymptotic stability of the desired distribution.

After providing some useful notation and mathematical preliminaries in Section II, we briefly recall the approach of [14] in Section III. Then, we assess the robustness properties of the continuification control approach in Sections IV and V. Finally, in Section VI, we show some preliminary results on the addition of an integral control action at the macroscopic level to improve the robustness of the microscopic dynamics, in the presence of perturbations or limited sensing. Theoretical results are illustrated by numerical simulations.

II. Mathematical preliminaries

Here, we offer some useful notation and mathematical concepts that will be used throughout the paper.

Definition 1 (Unit circle) *We define $\mathcal{S} := [-\pi, \pi]$ as the unit circle.*

Definition 2 (L^p-norm on $\mathcal{S}$ [15]) *Given a scalar function of $\mathcal{S}$ and time $h : \mathcal{S} \times \mathbb{R}_{\geq 0} \to \mathbb{R}$, we define its L^p-norm on $\mathcal{S}$ as*

$$\|h(\cdot, t)\|_p := \left(\int_{\mathcal{S}} |h(x,t)|^p \, \mathrm{d}x \right)^{1/p}. \tag{1}$$

For $p = \infty$,

$$\|h(\cdot, t)\|_\infty := \operatorname{ess\,sup}_{\mathcal{S}} |h(x,t)|. \tag{2}$$

For the sake of brevity, we denote these norms as $\|h\|_p$, without explicitly indicating their time dependencies.

This work has been partially supported by the National Science Foundation Grant No. CMMI-1932187 and by the Research Project SHARESPACE funded by the European Union (EU HORIZON-CL4-2022-HUMAN-01-14. SHARESPACE. GA 101092889 - http://sharespace.eu). Views and opinions expressed are however those of the author(s) only and do not necessarily reflect those of the European Union. The European Union cannot be held responsible for them.

[1]Scuola Superiore Meridionale, Naples, Italy
[2] Center for Urban Science and Progress, Department of Biomedical Engineering, Department of Mechanical and Aerospace Engineering, Tandon School of Engineering, New York University, USA
[3] Department of Electric Engineering and Information Technology, University of Naples Federico II, Naples, Italy
† These authors contributed equally
*For correspondence: mario.dibernardo@unina.it, mporfiri@nyu.edu

Lemma 1 (Holder's inequality [15]) *Given $f_1, \dots, f_n \in L^p$, we have*

$$\left\| \prod_{i=1}^{n} f_i \right\|_1 \leq \prod_{i=1}^{n} \|f_i\|_{p_i}, \quad \text{if} \quad \sum_{i=1}^{n} \frac{1}{p_i} = 1. \tag{3}$$

For instance, if $n = 2$, we have $\|f_1 f_2\|_1 \leq \|f_1\|_2 \|f_2\|_2$, as well as $\|f_1 f_2\|_1 \leq \|f_1\|_1 \|f_2\|_\infty$.

We denote with " $*$ " the convolution operator. When referring to periodic domains and functions, the operator needs to be interpreted as a circular convolution [16].

Lemma 2 (Young's convolution inequality [15]) *Given two functions, $f \in L^p$ and $g \in L^q$,*

$$\|f * g\|_r \leq \|f\|_p \, \|g\|_q, \quad \text{if} \quad \frac{1}{p} + \frac{1}{q} = \frac{1}{r} + 1, \tag{4}$$

where $1 \leq p, q, r \leq \infty$. For instance, $\|f * g\|_\infty \leq \|f\|_2 \|g\|_2$.

We denote time and space partial differentiation with the subscripts t and x, respectively. It can be shown [16] that the derivative of the convolution of two functions $(f * g)(x)$, can be computed as $(f * g)_x(x) = (f_x * g)(x) = (f * g_x)(x)$.

Lemma 3 (Comparison lemma [17]) *Given a scalar ordinary differential equation (ODE) $v_t = f(t, v)$, with $v(t_0) = v_0$, where f is continuous in t and locally Lipschitz in v, if a scalar function u fulfills the differential inequality*

$$u_t \leq f(t, u(t)), \quad u(t_0) \leq v_0, \tag{5}$$

then

$$u(t) \leq v(t), \quad \forall\, t \geq t_0. \tag{6}$$

III. Continuification control

As in [14], we consider a group of N identical mobile agents moving in $\mathcal{S}$. The dynamics of the i-th agent can be expressed as

$$\dot{x}_i = \sum_{j=1}^{N} f\left(\{x_i, x_j\}_\pi\right) + u_i, \tag{7}$$

where x_i is the angular position of agent i on $\mathcal{S}$, $\{x_i, x_j\}_\pi$ is the angular distance between agents i and j wrapped on $\mathcal{S}$, u_i is the velocity control input, and $f : \mathcal{S} \to \mathbb{R}$ is a periodic velocity interaction kernel modeling pairwise interactions between the agents. For a more detailed description, see [14].

Assuming the number of agents to be sufficiently large, the macroscopic collective dynamics can be adequately approximated through the mass balance equation [18]

$$\rho_t(x,t) + [\rho(x,t) V(x,t)]_x = q(x,t), \tag{8}$$

where $\rho : \mathcal{S} \times \mathbb{R}_{\geq 0} \to \mathbb{R}_{\geq 0}$ is the density profile of the agents on $\mathcal{S}$ at t such that $\int_{\mathcal{S}} \rho(x,t)\, \mathrm{d}x = N$ for any t, and V is the velocity field, which can be expressed as

$$V(x,t) = \int_{-\pi}^{\pi} f\left(\{x, y\}_\pi\right) \rho(y,t)\, \mathrm{d}y = (f * \rho)(x,t), \tag{9}$$

with the function f encapsulating all-to-all interactions in the continuum. The function q represents the macroscopic control input, which we first write as a mass source/sink to simplify derivations, but then recast as a velocity field.

The boundary and initial conditions are given as follows:

$$\rho(-\pi, t) = \rho(\pi, t), \quad \forall t \geq 0, \tag{10}$$

$$\rho(x, 0) = \rho^0(x), \quad \forall x \in \mathcal{S}. \tag{11}$$

We remark that V is periodic by construction, as it comes from a circular convolution. This ensures that, in the open-loop scenario, when $q = 0$, mass is conserved, that is $\mathrm{d}/\mathrm{d}t \int_{\mathcal{S}} \rho(x,t)\, \mathrm{d}x = 0$ (integrating by parts).

Given some desired periodic smooth density profile, $\rho^{\mathrm{d}}(x,t)$, associated with the target agents' configuration, and such that $\|\rho^{\mathrm{d}}\|_2 \leq M$ and $\|\rho^{\mathrm{d}}_x\|_2 \leq L$ at any t, the continuification control problem is that of finding the control inputs $u_i,\ i = 1, 2, \dots, N$ in (7) such that

$$\lim_{t \to \infty} \|\rho^{\mathrm{d}}(\cdot, t) - \rho(\cdot, t)\|_2 = 0, \tag{12}$$

for agents starting from any initial configuration $x_i(0) = x_{i0},\ i = 1, \dots, N$.

To solve this problem, we first choose q in (8) as

$$q(x,t) = K_{\mathrm{p}} e(x,t) - \left[e(x,t) V^{\mathrm{d}}(x,t)\right]_x - \left[\rho(x,t) V^{\mathrm{e}}(x,t)\right]_x, \tag{13}$$

where K_{p} is a positive control gain, $e = \rho^{\mathrm{d}} - \rho$, $V^{\mathrm{d}} = (f * \rho^{\mathrm{d}})$, $V^{\mathrm{e}} = (f * e)$, and we consider the reference dynamics

$$\rho^{\mathrm{d}}_t(x,t) + \left[\rho^{\mathrm{d}}(x,t) V^{\mathrm{d}}(x,t)\right]_x = 0, \tag{14}$$

fulfilling initial and boundary conditions similar to those of (8), namely (10) and (11). As shown in [14], this ensures that the density ρ globally asymptotically converges to ρ^{d}.

Then, we recast the macroscopic controlled model (8) to include q as a control action on the velocity field, that is,

$$\rho_t(x,t) + [\rho(x,t)(V(x,t) + U(x,t))]_x = 0, \tag{15}$$

where U is an auxiliary function computed from the linear PDE

$$[\rho(x,t) U(x,t)]_x = -q(x,t). \tag{16}$$

Integrating (16), we obtain (assuming $\rho \neq 0$)

$$U(x,t) = -\frac{1}{\rho(x,t)} \left[\int q(y,t)\, \mathrm{d}y + q(-\pi, t) \right]. \tag{17}$$

Finally, we compute the velocity input acting on agent i at the microscopic level by spatially sampling U at x_i

$$u_i(t) = U(x_i, t), \quad i = 1, 2, \dots N. \tag{18}$$

The main limitation of this approach is the non-local nature of the control action. Since (13) is based on the convolution V^{e}, agent i must have global knowledge of e to compute u_i. Moreover, as the choice of q is based on some cancellations of the macroscopic dynamics of the system, the robustness to structural perturbations needs to be properly assessed. In this study, we address both of these issues.

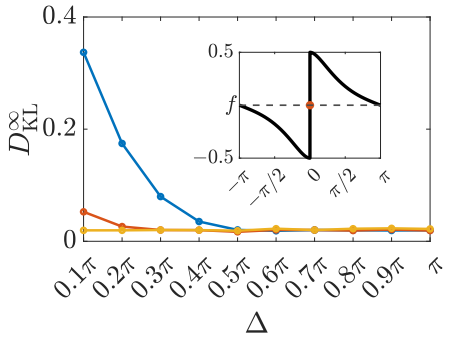

Fig. 1: Steady-state value of the KL divergence, D_{KL}^{∞} at the end of a monomodal regulation trial, for different values of Δ and K_{p} ($K_{\mathrm{p}} = 10$ in blue, $K_{\mathrm{p}} = 100$ in orange and $K_{\mathrm{p}} = 1000$ in yellow). In the inset, we show the repulsive interaction kernel used in the simulations.

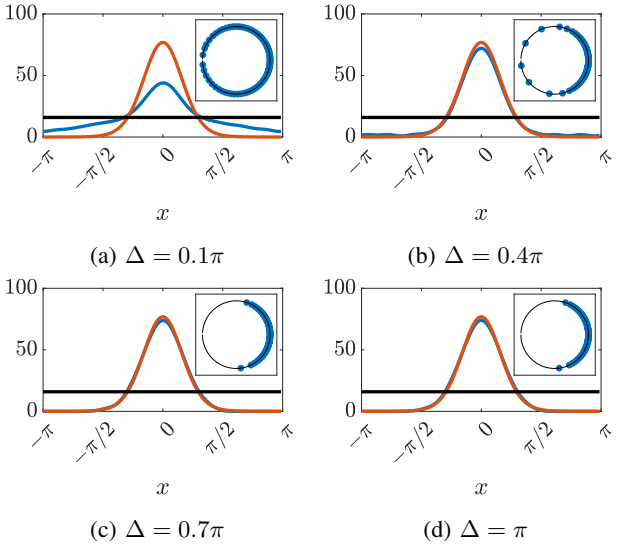

(a) $\Delta = 0.1\pi$ (b) $\Delta = 0.4\pi$

(c) $\Delta = 0.7\pi$ (d) $\Delta = \pi$

Fig. 2: Steady-state ($t = t_{\mathrm{f}}$) comparison between the agents distribution (blue line) and the desired one (orange line) when the agents are started from the initial distribution shown as a black line, for increasing sensing abilities of the agents when $K_{\mathrm{p}} = 10$. Panel (d) shows the case when sensing is unlimited. In the inset of each panel, we display the discrete formation of the agents at the end of the trial.

IV. Limited sensing capabilities

To relax the assumption of unlimited sensing, we assume agents can only sense an interval $[-\Delta, \Delta]$, with $\Delta > 0$ centered at their position. Then, the macroscopic control action in (13) becomes

$$\hat{q}(x,t) = K_{\mathrm{p}} e(x,t) - \left[e(x,t)V^{\mathrm{d}}(x,t)\right]_x - \left[\rho(x,t)\widehat{V}^{\mathrm{e}}(x,t)\right]_x, \quad (19)$$

where $\widehat{V}^{\mathrm{e}} = (\hat{f} * e)$, and $\hat{f}$ is a modified velocity interaction kernel defined as

$$\hat{f}(z) = f(z)\Pi(z,\Delta), \quad (20)$$

with $\Pi(z,\Delta)$ being the rectangular window of size 2Δ

$$\Pi(z,\Delta) = \begin{cases} 1 & \text{if } |z| \le \Delta, \\ 0 & \text{otherwise.} \end{cases} \quad (21)$$

Using $\hat{q}$ instead of q as input to the macroscopic model (8) yields the following error dynamics:

$$e_t(x,t) = -K_{\mathrm{p}} e(x,t) + \left[\rho^{\mathrm{d}}(x,t)\tilde{V}(x,t)\right]_x - \left[e(x,t)\tilde{V}(x,t)\right]_x, \quad (22)$$

where $\tilde{V} = (g * e)$ with $g := \hat{f} - f$.

Theorem 1 (Stability under limited sensing) *The control strategy* (19) *achieves semiglobal stabilization of the error system* (22) *so that, for any initial condition in a compact set $\|e(\cdot,0)\|_2 < \gamma$ with $\gamma > 0$, choosing K_{p} sufficiently large ensures the error converges asymptotically to 0.*

Proof: Choosing $\|e\|_2^2$ as a candidate Lyapunov function for (22), we get (omitting dependencies for simplicity)

$$(\|e\|_2^2)_t = 2\int_{\mathcal{S}} e e_t \,\mathrm{d}x = -2K_{\mathrm{p}}\|e\|_2^2 - \int_{\mathcal{S}} e^2 \tilde{V}_x \,\mathrm{d}x + 2\int_{\mathcal{S}} (e\rho_x^{\mathrm{d}}\tilde{V} + e\rho^{\mathrm{d}}\tilde{V}_x)\,\mathrm{d}x, \quad (23)$$

where we computed product derivatives and used integration by parts taking into account the periodicity of the functions. Using the definition of L^1-norm (see Definition 2), applying Holder's inequality with $n = 3$, $p_1 = p_2 = 2$, and $p_3 = \infty$ (see Lemma 1), invoking Young's convolution inequality with $r = \infty$ and $p = q = 2$ (see Lemma 2), and recalling the assumption on the L^2- boundedness of ρ^{d} and ρ_x^{d} by constants L and M, we find

$$\left|\int_{\mathcal{S}} e\rho_x^{\mathrm{d}}\tilde{V}\,\mathrm{d}x\right| \le \int_{\mathcal{S}} |e\rho_x^{\mathrm{d}}\tilde{V}|\,\mathrm{d}x = \|e\rho_x^{\mathrm{d}}\tilde{V}\|_1 \le \le \|e\|_2\|\rho_x^{\mathrm{d}}\|_2\|\tilde{V}\|_\infty \le L\|e\|_2^2\|g\|_2, \quad (24)$$

$$\left|\int_{\mathcal{S}} e\rho^{\mathrm{d}}\tilde{V}_x\,\mathrm{d}x\right| \le \int_{\mathcal{S}} |e\rho^{\mathrm{d}}\tilde{V}_x|\,\mathrm{d}x = \|e\rho^{\mathrm{d}}\tilde{V}_x\|_1 \le \le \|e\|_2\|\rho^{\mathrm{d}}\|_2\|\tilde{V}_x\|_\infty \le M\|e\|_2^2\|g_x\|_2, \quad (25)$$

$$\left|\int_{\mathcal{S}} e^2\tilde{V}_x\,\mathrm{d}x\right| \le \int_{\mathcal{S}} |e^2\tilde{V}_x|\,\mathrm{d}x = \|ee\tilde{V}_x\|_1 \le \le \|e\|_2^2\|\tilde{V}_x\|_\infty \le \|e\|_2^3\|g_x\|_2. \quad (26)$$

Using these bounds, from (23) we can write

$$(\|e\|_2^2)_t \le (-2K_{\mathrm{p}} + 2M\|g_x\|_2 + 2L\|g\|_2 + \|g_x\|_2\|e\|_2)\|e\|_2^2. \quad (27)$$

Then, choosing $K_{\mathrm{p}} > (M + \gamma/2)\|g_x\|_2 + L\|g\|_2$, guarantees that the error asymptotically tends to 0; thus proving semiglobal stability[1]. ■

We remark that (i) as Δ becomes smaller, $\|g\|_2$ and $\|g_x\|_2$ increase, requiring a larger value of K_{p} to ensure convergence, and (ii) in the limit of local dynamics about the

[1]Theorem 1 in [14] should be equivalently interpreted.

origin, where we neglect cubic terms in e, one can choose $K_{\mathrm{p}} = M\|g_x\|_2 + L\|g\|_2$.

Numerical validation: We consider the same framework, control discretization and numerical set-up as in [14]. In particular, we refer to a mono-modal regulation scenario, where a repulsive swarm of $N = 100$ agents, starting evenly displaced in $\mathcal{S}$, is required to achieve a desired density profile given by a von Mises function, with mean $\mu = 0$ and concentration coefficient $k = 4$. The pairwise interactions between agents is modelled via a repulsive Morse potential, depicted in the inset of Fig. 1, given by

$$f(x) = \mathrm{sign}(x)\left[-G\mathrm{e}^{-|x|/L} + \mathrm{e}^{-|x|}\right], \qquad (28)$$

where the characteristic parameters, modulating the strength and characteristic distance of the attractive term, are $G = L = 0.5$, making the repulsion term dominant.

We run several trials of duration $t_{\mathrm{f}} = 6$. In each trial, we consider a different sensing radius Δ, spanning from 0.1π to π. At the end of each trial, we record the steady-state Kullback-Leibler (KL) divergence , D_{KL}^{∞}, between $\hat{\rho}$ and $\hat{\rho}^{\mathrm{d}}$ (equivalent to ρ and ρ^{d}, but normalized to sum to 1) [19]. The results of such a numerical investigation are reported in Fig. 1, for different values of K_{p}. They show that: (i) for large values of K_{p}, performance is independent from the specific sensing radius that is given to the agents, and (ii) for smaller values of K_{p}, a limited knowledge of the domain can still guarantee a performance level that is comparable to the case of $\Delta = \pi$. For example, when considering $K_{\mathrm{p}} = 10$, choosing $\Delta = 0.4\pi$ makes D_{KL}^{∞} comparable to the value obtained for unlimited sensing capabilities. We also report in Fig. 2 the final configuration of the swarm for different values of the sensing radius, when $K_{\mathrm{p}} = 10$. We remark that the non-zero D_{KL}^{∞} comes from the discretization process, and it approaches 0 in the limit of an infinite number agents.

V. Structural perturbations

Next, we assess the robustness of the approach to two classes of perturbations, the first acting additively on the macroscopic velocity field and the second on the interaction kernel.

A. Spatio-temporal perturbations of the velocity field

We assume that perturbations of the microscopic dynamics can be captured at the macroscopic level by means of some spatio-temporal velocity field $d(x,t)$ affecting (8). The macroscopic controlled model becomes

$$\rho_t(x,t) + [\rho(x,t)(V(x,t) + d(x,t))]_x = q(x,t), \qquad (29)$$

where we assume $d(-\pi,t) = d(\pi,t)$ for any t and $d, d_x \in L^{\infty}$ at any t so that that there exist two positive constants D_1 and D_2 bounding the L^{∞}-norm of d and d_x, respectively.

Substituting (13) into (29) and taking into account the reference dynamics (14) yields

$$e_t(x,t) = -K_{\mathrm{p}} e(x,t) + \left[(\rho^{\mathrm{d}}(x,t) - e(x,t))d(x,t)\right]_x. \qquad (30)$$

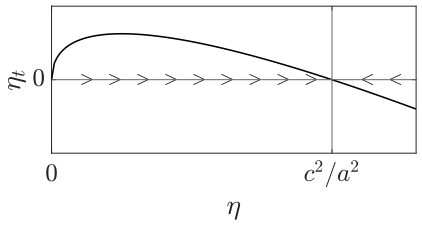

Fig. 3: Phase portrait of system (36), bounding $\|e\|_2^2$ in the presence of spatio-temporal disturbances.

Theorem 2 (Bounded convergence in the presence of velocity perturbations) *There exists a threshold value $D_2 < \kappa < +\infty$ such that, if $2K_{\mathrm{p}} > \kappa$, the dynamics of the squared error norm is bounded and*

$$\limsup_{t\to\infty} \|e(\cdot,t)\|_2 \leq \frac{2LD_1 + 2MD_2}{\kappa - D_2}$$

Hence, the upper bound on the steady-state error can be made arbitrarily small by choosing κ sufficiently large.

Proof: Taking into account (30), we write the dynamics of $\|e\|_2^2$ (omitting dependencies for simplicity) as

$$(\|e\|_2^2)_t = 2\int_{\mathcal{S}} e e_t \,\mathrm{d}x = -2K_{\mathrm{p}}\|e\|_2^2 - \int_{\mathcal{S}} e^2 d_x \,\mathrm{d}x + 2\int_{\mathcal{S}} (e\rho_x^{\mathrm{d}} d + e\rho^{\mathrm{d}} d_x)\,\mathrm{d}x, \qquad (31)$$

where we computed product derivatives and applied integration by parts exploiting the periodicity of the functions. Similarly to the proof of Theorem 1, we apply Definition 2, Holder's inequality with $n = 3$, $p_1 = p_2 = 2$ and $p_3 = \infty$ (see Lemma 1), and exploit the bounds on ρ^{d}, ρ_x^{d}, d and d_x, to derive the following inequalities for the terms in (31):

$$\left|\int_{\mathcal{S}} e\rho_x^{\mathrm{d}} d\,\mathrm{d}x\right| \leq \int_{\mathcal{S}} |e\rho_x^{\mathrm{d}} d|\,\mathrm{d}x = \|e\rho_x^{\mathrm{d}} d\|_1 \leq \leq \|e\|_2\|\rho_x^{\mathrm{d}}\|_2\|d\|_{\infty} \leq LD_1\|e\|_2, \qquad (32)$$

$$\left|\int_{\mathcal{S}} e\rho^{\mathrm{d}} d_x\,\mathrm{d}x\right| \leq \int_{\mathcal{S}} |e\rho^{\mathrm{d}} d_x|\,\mathrm{d}x = \|e\rho^{\mathrm{d}} d_x\|_1 \leq \leq \|e\|_2\|\rho^{\mathrm{d}}\|_2\|d_x\|_{\infty} \leq MD_2\|e\|_2, \qquad (33)$$

$$\left|\int_{\mathcal{S}} e^2 d_x\,\mathrm{d}x\right| \leq \int_{\mathcal{S}} |e^2 d_x|\,\mathrm{d}x = \|eed_x\|_1 \leq \leq \|e\|_2^2\|d_x\|_{\infty} \leq D_2\|e\|_2^2. \qquad (34)$$

Hence, we obtain

$$(\|e\|_2^2)_t \leq (-2K_{\mathrm{p}} + D_2)\,\|e\|_2^2 + (2LD_1 + 2MD_2)\,\|e\|_2. \qquad (35)$$

For convenience, we rewrite (35) as

$$\eta_t \leq -a\eta + c\sqrt{\eta} := h(\eta), \qquad (36)$$

where $\eta = \|e\|_2^2$, $a = 2K_{\mathrm{p}} - D_2$, and $c = 2LD_1 + 2MD_2$. Under the assumption that $2K_{\mathrm{p}} > D_2$ ($a > 0$), the phase

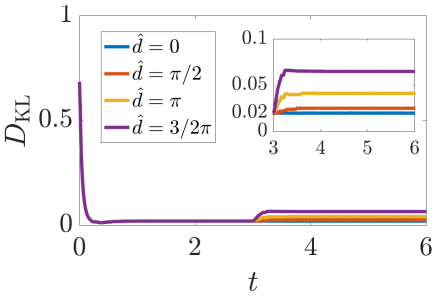

Fig. 4: Time evolution of the KL divergence when a constant disturbance of amplitude $\hat{d}$ switches on at $t = 3$. In the inset, a zoom of the second half of the trial is given.

portrait of the bounding field h yield an asymptotically stable equilibrium at (see Fig. 3)

$$\frac{c^2}{a^2} = \frac{(2LD_1 + 2MD_2)^2}{(2K_\mathrm{p} - D_2)^2}$$

(with basin of attraction $\mathbb{R}_{>0}$). Thus, using Lemma 3, η is bounded by c^2/a^2. Moreover, choosing $2K_\mathrm{p} > \kappa > D_2$, the stable equilibrium of the bounding field h can be moved arbitrarily closer to the origin. ■

Numerical validation: We consider the same scenario presented in the previous section but assuming that a disturbance $d(x,t) = \hat{d}\, w(t)$, where $\hat{d}$ is a constant and $w(t) = \mathrm{step}(t - t_\mathrm{f}/2)$, is acting on the macroscopic dynamics. Setting $K_\mathrm{p} = 10$ and considering different values of $\hat{d}$, we obtain the results reported in Fig. 4. As expected, in the presence of the disturbance, the KL divergence remains bounded and decreases as the control gain K_p increases. For example, the steady-state value of the KL divergence decreases from 0.06 when $K_\mathrm{p} = 10$ to less than 0.02 when $K_\mathrm{p} \geq 100$.

B. Interaction kernel perturbation

Next, we consider the case where structural perturbations affect the interaction kernel. We assume that the interaction kernel, $\tilde{f}$, used to compute the macroscopic control action is different from the actual interaction kernel, f, influencing the agents' motion. We compute the control input as

$$\tilde{q}(x,t) = K_\mathrm{p} e(x,t) - \Big[e(x,t)\tilde{V}^\mathrm{d}(x,t)\Big]_x - \Big[\rho(x,t)\tilde{V}^\mathrm{e}(x,t)\Big]_x, \quad (37)$$

where $\tilde{V}^\mathrm{d} = (\tilde{f} * \rho^\mathrm{d})$ and $\tilde{V}^\mathrm{e} = (\tilde{f} * e)$.

Substituting (37) into (8) and considering the reference dynamics (14), the error dynamics becomes

$$e_t(x,t) = -K_\mathrm{p} e(x,t) + \Big[e(x,t)\tilde{U}^\mathrm{d}(x,t)\Big]_x + \Big[\rho^\mathrm{d}(x,t)\tilde{U}^\mathrm{e}(x,t)\Big]_x - \Big[e(x,t)\tilde{U}^\mathrm{e}(x,t)\Big]_x, \quad (38)$$

where, letting $\tilde{g} = \tilde{f} - f$ be the mismatch between the interaction kernels, we have

$$\tilde{U}^\mathrm{d}(x,t) = \tilde{V}^\mathrm{d}(x,t) - V^\mathrm{d}(x,t) = (\tilde{g} * e)(x,t), \quad (39)$$

$$\tilde{U}^\mathrm{e}(x,t) = \tilde{V}^\mathrm{e}(x,t) + V^\mathrm{e}(x,t) = (\tilde{g} * e)(x,t). \quad (40)$$

Theorem 3 (Stability with kernel perturbation) *For any positive γ and initial condition $e(x,0)$ in the compact set $\|e(\cdot,0)\|_2 < \gamma$, if K_p is sufficiently large then* (38) *asymptotically converges to 0.*

Proof: Assuming $\|e\|_2^2$ to be a candidate Lyapunov function for (38), we get

$$(\|e\|_2^2)_t = \int_\mathcal{S} e e_t \,\mathrm{d}x = -2K_\mathrm{p}\|e\|_2^2 - \int_\mathcal{S} e^2 \tilde{U}^\mathrm{e}_x \,\mathrm{d}x + \int_\mathcal{S} e^2 \tilde{U}^\mathrm{d}_x \,\mathrm{d}x - 2\int_\mathcal{S} (e\rho^\mathrm{d}_x \tilde{U}^\mathrm{e} + e\rho^\mathrm{d}\tilde{U}^\mathrm{e}_x)\,\mathrm{d}x. \quad (41)$$

where we computed the product derivatives and used integration by parts by exploiting the fact that $\tilde{U}^\mathrm{d}$ and $\tilde{U}^\mathrm{e}$ are periodic by construction (they come from a circular convolution). Using similar arguments to those above, we can establish upper bounds for the terms in (41) as follows:

$$\left|\int_\mathcal{S} e\rho^\mathrm{d}_x \tilde{U}^\mathrm{e}\,\mathrm{d}x\right| \leq \int_\mathcal{S} |e\rho^\mathrm{d}_x \tilde{U}^\mathrm{e}|\,\mathrm{d}x = \|e\rho^\mathrm{d}_x \tilde{U}^\mathrm{e}\|_1 \leq \leq \|e\|_2\|\rho^\mathrm{d}_x\|_2\|\tilde{U}^\mathrm{e}\|_\infty \leq L\|\tilde{g}\|_2\|e\|_2^2, \quad (42)$$

$$\left|\int_\mathcal{S} e\rho^\mathrm{d}\tilde{U}^\mathrm{e}_x\,\mathrm{d}x\right| \leq \int_\mathcal{S} |e\rho^\mathrm{d}\tilde{U}^\mathrm{e}_x|\,\mathrm{d}x = \|e\rho^\mathrm{d}\tilde{U}^\mathrm{e}_x\|_1 \leq \leq \|e\|_2\|\rho^\mathrm{d}\|_2\|\tilde{U}^\mathrm{e}_x\|_\infty \leq M\|\tilde{g}_x\|_2\|e\|_2^2, \quad (43)$$

$$\left|\int_\mathcal{S} e^2\tilde{U}^\mathrm{e}_x\,\mathrm{d}x\right| \leq \int_\mathcal{S} |e^2\tilde{U}^\mathrm{e}_x|\,\mathrm{d}x = \|ee\tilde{U}^\mathrm{e}_x\|_1 \leq \leq \|e\|_2^2\|\tilde{U}^\mathrm{e}_x\|_\infty \leq \|\tilde{g}_x\|_2\|e\|_2^3, \quad (44)$$

$$\left|\int_\mathcal{S} e^2\tilde{U}^\mathrm{d}_x\,\mathrm{d}x\right| \leq \int_\mathcal{S} |e^2\tilde{U}^\mathrm{d}_x|\,\mathrm{d}x = \|ee\tilde{U}^\mathrm{d}_x\|_1 \leq \leq \|e\|_2^2\|\tilde{U}^\mathrm{d}_x\|_\infty \leq \|e\|_2^2\|\|\rho^\mathrm{d}\|_2\|\tilde{g}_x\|_2 \leq M\|\tilde{g}_x\|_2\|e\|_2^2. \quad (45)$$

Using these bounds in (41) we obtain

$$(\|e\|_2^2)_t \leq (-2K_\mathrm{p} + 3M\|\tilde{g}_x\|_2 + 2L\|\tilde{g}\|_2 + \|\tilde{g}_x\|_2\|e\|_2)\|e\|_2^2. \quad (46)$$

Then, choosing $K_\mathrm{p} > \|\tilde{g}_x\|_2\gamma/2 + 3M\|\tilde{g}_x\|_2/2 + L\|\tilde{g}\|_2$ ensures the convergence of the error to 0. ■

Note that, in the limit of local analysis, where we neglect cubic terms in e, $K_\mathrm{p} = 3M\|\tilde{g}_x\|_2/2 + L\|\tilde{g}\|_2$.

Numerical validation: We consider again the scenario used in Section IV but we assume that a perturbed kernel is used to compute the macroscopic control action q. Specifically, we test robustness against the two perturbed kernels $\tilde{f}_1$ and $\tilde{f}_2$, obtained by setting the characteristic parameters in (28) to $G = L = 0.1$ and $G = L = 0.9$, respectively.

Setting $K_\mathrm{p} = 10$, we obtain results shown in Fig. 5 where we observe an increase in the steady-state mismatch between the distribution of the agents and the desired density as the kernel becomes more different than the nominal one ($\tilde{f}_2$ being the worst case). Our numerical results confirm

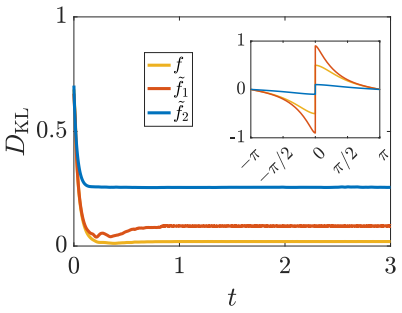

Fig. 5: Time evolution of the KL divergence when the perturbed kernels $\tilde{f}_1$ and $\tilde{f}_2$ shown in the inset are used to compute the control action, instead of the nominal kernel f.

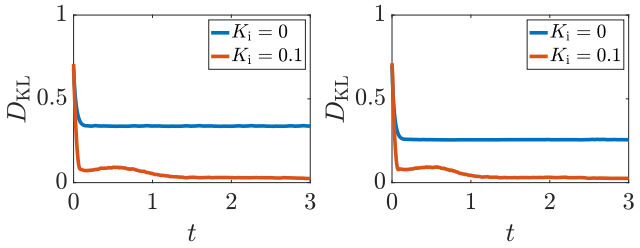

(a) (b)

Fig. 6: Effects of a macroscopic integral action when (a) agents possess limited sensing with $\Delta = 0.1\pi$ and (b) when their interaction kernel is perturbed and set equal to $\tilde{f}_2$. We compare the cases of $K_{\mathrm{i}} = 0$ and $K_{\mathrm{i}} = 0.1$, for $K_{\mathrm{p}} = 10$.

that the steady-state mismatch decreases as K_{p} increases. Specifically, choosing $K_{\mathrm{p}} > 100$, yields a value of D_{KL}^{∞} lower than 0.05.

VI. Adding a Macroscopic Integral Action

In all the examined cases, some bounded mismatch between the desired and steady-state distribution of the agents remains, especially when K_{p} is low. To resolve this issue, we explored the addition to the macroscopic control law in (13) of an integral action $K_{\mathrm{i}} \int_0^{\tau} e(x,\tau)\,\mathrm{d}\tau$, with K_{i} being a positive control gain. Such a modified control action is then descretized as in (18). We observe that the resulting control strategy still ensures convergence, while reducing the steady-state error due to discretization and the presence of perturbations. (See Fig. 6 for some representative cases.)

These findings suggest the advantages of adding an integral action to compensate for disturbances and perturbations within a continuification-based control strategy.

VII. Conclusions

We investigated the stability and robustness properties of a continuification control strategy for a set of agents in a ring. We quantified the extent to which the approach presented in [14] is affected by (i) limited sensing capabilities of the agents; (ii) presence of spatio-temporal disturbances; and (iii) structural perturbations of the interaction kernel. In all cases, we establish the mathematical proofs of semiglobal asymptotic or bounded convergence – the latter in the form of a residual steady-state mismatch that can be made arbitrarily small by increasing the control gain. We also reported preliminary results about the addition of a spatio-temporal integral action at the macroscopic level.

References

[1] D. Nikitin, C. Canudas-de Wit, and P. Frasca, "A continuation method for large-scale modeling and control: From odes to pde, a round trip," *IEEE Transactions on Automatic Control*, vol. 67, no. 10, pp. 5118–5133, 2022.

[2] M. di Bernardo, "Controlling collective behavior in complex systems," in *Encyclopedia of Systems and Control*, J. Baillieul and T. Samad, Eds. Springer London, 2020.

[3] G. Freudenthaler and T. Meurer, "Pde-based multi-agent formation control using flatness and backstepping: Analysis, design and robot experiments," *Automatica*, vol. 115, p. 108897, 2020.

[4] S. Biswal, K. Elamvazhuthi, and S. Berman, "Decentralized control of multiagent systems using local density feedback," *IEEE Transactions on Automatic Control*, vol. 67, no. 8, pp. 3920–3932, 2021.

[5] J. Qi, R. Vazquez, and M. Krstic, "Multi-agent deployment in 3-d via pde control," *IEEE Transactions on Automatic Control*, vol. 60, no. 4, pp. 891–906, 2014.

[6] C. Sinigaglia, A. Manzoni, and F. Braghin, "Density control of large-scale particles swarm through pde-constrained optimization," *IEEE Transactions on Robotics*, vol. 38, no. 6, pp. 3530–3549, 2022.

[7] A. Guarino, D. Fiore, D. Salzano, and M. di Bernardo, "Balancing cell populations endowed with a synthetic toggle switch via adaptive pulsatile feedback control," *ACS Synthetic Biology*, vol. 9, no. 4, pp. 793–803, 2020.

[8] D. K. Agrawal, R. Marshall, V. Noireaux, and E. D. Sontag, "In vitro implementation of robust gene regulation in a synthetic biomolecular integral controller," *Nature Communications*, vol. 10, no. 1, pp. 1–12, 2019.

[9] A. Rubio Denniss, T. E. Gorochowski, and S. Hauert, "An open platform for high-resolution light-based control of microscopic collectives," *Advanced Intelligent Systems*, p. 2200009, 2022.

[10] T. Menara, G. Baggio, D. Bassett, and F. Pasqualetti, "Functional control of oscillator networks," *Nature Communications*, vol. 13, no. 1, p. 4721, 2022.

[11] R. Noori, D. Park, J. D. Griffiths, S. Bells, P. W. Frankland, D. Mabbott, and J. Lefebvre, "Activity-dependent myelination: A glial mechanism of oscillatory self-organization in large-scale brain networks," *Proceedings of the National Academy of Sciences*, vol. 117, no. 24, pp. 13 227–13 237, 2020.

[12] S. Shahal, A. Wurzberg, I. Sibony, H. Duadi, E. Shniderman, D. Weymouth, N. Davidson, and M. Fridman, "Synchronization of complex human networks," *Nature communications*, vol. 11, no. 1, pp. 1–10, 2020.

[13] C. Calabrese, M. Lombardi, E. Bollt, P. De Lellis, B. G. Bardy, and M. Di Bernardo, "Spontaneous emergence of leadership patterns drives synchronization in complex human networks," *Scientific Reports*, vol. 11, no. 1, pp. 1–12, 2021.

[14] G. C. Maffettone, A. Boldini, M. Di Bernardo, and M. Porfiri, "Continuification control of large-scale multiagent systems in a ring," *IEEE Control Systems Letters*, vol. 7, pp. 841–846, 2023.

[15] S. Axler, *Measure, integration & real analysis*. Springer Nature, 2020.

[16] M. C. Jeruchim, P. Balaban, and K. S. Shanmugan, *Simulation of communication systems: modeling, methodology and techniques*. Springer Science & Business Media, 2006.

[17] H. K. Khalil, *Nonlinear systems*. Patience Hall, 2002.

[18] A. J. Bernoff and C. M. Topaz, "A primer of swarm equilibria," *SIAM Journal on Applied Dynamical Systems*, vol. 10, no. 1, pp. 212–250, 2011.

[19] S. Kullback and R. A. Leibler, "On information and sufficiency," *The Annals of Mathematical Statistics*, vol. 22, no. 1, pp. 79–86, 1951.